# Shot noise and tunneling magnetoresistance in disordered MgO-based double-barrier magnetic tunnel junctions: First-principles study

Junting Yang,[1,2,3] Jiawei Yan,[1,2,3] Shizhuo Wang,[4] and Youqi Ke[1,2,3,*]

[1]*Shanghai Institute of Optics and Fine Mechanics, Chinese Academy of Sciences, Shanghai 201800, China*

[2]*Division of Condensed Matter Physics and Photonic Science, School of Physical Science and Technology, ShanghaiTech University, Shanghai 201210, China*

[3]*University of Chinese Academy of Sciences, Beijing 100049, China*

[4]*College of Physics and Electronic Engineering, Zhengzhou University of Light Industry, Zhengzhou 450002, China*

(Received 29 November 2017; revised manuscript received 22 March 2018; published 21 May 2018)

We report first-principles study of shot noise and tunneling magnetoresistance in Fe/MgO/Fe- /MgO/Fe double-barrier magnetic tunnel junctions (MTJs). We mainly investigate the effects of disordered interfacial oxygen vacancies and barrier asymmetry on the spin-dependent tunneling. It is found that interchannel scattering induced by interfacial oxygen vacancies can substantially enhance the tunneling conductance of the antiparallel magnetic configurations, and results in the dramatic decrease of tunneling magnetoresistance. Moreover, we find the interfacial disorder scattering favors the sub-Poissonian tunneling process. As a result, Fano factors of symmetric MTJs maintain at around 0.5, or are suppressed, while Fano factors of asymmetric MTJs can all be significantly suppressed, illustrating the important correlations in tunneling induced by interfacial disorders. Interchannel scattering induced by interfacial oxygen vacancies can effectively couple the electron to high-transmission channels, enhancing the transmission and reducing the shot noise. In comparison with interfacial disorder, middle-layer disordered Fe vacancies present limited modulation on the Fano factor. Increasing the asymmetry of barriers can quickly decrease high-transmission channels, and make the tunneling process Poissonian in double-barrier MTJs.

DOI: 10.1103/PhysRevB.97.174420

## I. INTRODUCTION

The tunneling magnetoresistance (TMR) effect is one of the most important spintronic phenomena featuring important applications in magnetic sensors, magnetic random access memory, etc. [1–5]. It is well known that the MgO based single-barrier (SB) magnetic tunneling junctions (MTJs), FM/MgO/FM (FM denotes ferromagnetic material), possess a giant TMR effect due to the important spin-filtering effect of the device [6]. Besides single barrier MTJs, MgO based double-barrier (DB) MTJs, FM/MgO/FM/MgO/FM, have also received much attention due to their interesting transport physics and important potential applications. In particular, in comparison with the SBMTJ, MgO based DBMTJ features a spin dependent resonant tunneling effect [7–13], more resistance states, reduced bias dependence of TMR [14–18], enhanced current density and spin-transfer torque effects [19–21], and enhanced TMR [22–24], as well as the controllable noise-to-signal ratio [25,26], which are desirable for practical applications. Therefore, the understanding of the spin-dependent tunneling mechanism in DBMTJs is important for both technology and fundamental physics.

However, due to the stochastic nature of quantum transport, understanding of the transport mechanisms at nanoscale requires transport statistics, which is usually measured by a set of cumulants including time-averaged current, shot noise, and skewness, etc. In most cases, only first-order cumulant and related properties including conductance or $I$-$V$ characteristics, TMR ratio, and spin transfer torque are studied to demonstrate various physical effects on the transport, while the simulation and measurement of the higher-order cumulants are very challenging for realistic nanoelectronics. The second cumulant shot noise, measuring quantum fluctuation of the current, is not only important for applications, but also provides important information about the nature of transport channels, unit of transferred charge, and other diagnostic information. (For reviews, see Refs. [27,28].) Without correlations, the transport can be described by the Poissonian process with shot noise $S_{\text{poisson}} = 2eI$. The deviation from the Poissonian noise, measured by the Fano factor $F = S/2eI$, reflects the coherency and correlations of electrons, which are not accessible by the time-averaged current. Therefore, having both the current/conductance and shot noise is crucial for analyzing the spin-dependent tunneling mechanism in DBMTJs. It has been experimentally demonstrated that the TMR and shot noise in DBMTJs shows important dependence on the magnetic configurations and the asymmetry of the MgO barriers [11,29], reflecting their important effects on the spin-dependent tunneling statistics [25]. As far as we know, to fit the experimental measurements, a phenomenological model has been proposed with a couple of tunable parameters for DBMTJs [26]. However, how the realistic factors affect the spin-dependent tunneling in DBMTJs is still unknown, especially the prominent effects of the inevitable disordered impurities/defects. For the MgO-based SBMTJs, previous studies

*keyq@shanghaitech.edu.cn

 

have demonstrated that the disorders, including oxidation and oxygen vacancies, etc., do have significant influence on the spin dependent tunneling [30–38]. The first-principles simulation of shot noise in MgO based SBMTJs has demonstrated that the interfacial disorders can significantly modulate the tunneling statistics in the minority spin channel of the parallel magnetic state in junction with a thin MgO barrier, while all the other spin channels maintain a nearly Poissonian tunneling process [39,40]. However, DBMTJs possesses distinct tunneling statistics from SBMTJs, for example, symmetric DBTJs usually feature $F = 0.5$ with a significantly sub-Poissonian tunneling process, while SBTJs are mostly dominated by the Poissonian process [26,27]. Experimentally, it has been reported that the TMR of MgO-based DBMTJs can be significantly affected by different annealing temperature [17,18]. Although there are already many important theoretical studies on the tunneling physics in DBMTJs, the important effects of disorders on the spin dependent tunneling statistics remain largely unexplored for DBMTJs. Therefore, it is important to study the effects of different realistic factors on the tunneling magnetoresistance and shot noise in DBMTJs.

However, to analyze the transport statistics of the realistic device with atomic disorders, the disorder average over the transmission and shot noise is indispensable, and presents a great challenge for the first-principles quantum transport method. Aiming at solving this problem, three of the authors have reported a first-principles generalized nonequilibrium vertex correction (NVC) in coherent medium theory for simulating quantum transport through disordered nanodevices [41–43]. In this method, based on carrying out coherent potential approximation (CPA) [44,45] to the Keldysh nonequilibrium Green's function (GF), a generalized nonequilibrium vertex correction is developed to account for multiple impurity scattering in the disorder averaged two-GF correlators [41–43]. For the quantum transport through nanoscale devices, it is known that the current and shot-noise power are given by (at zero temperature) [27]

$$I = \frac{e}{h}\int_{\mu_R}^{\mu_L} \mathrm{Tr}[\hat{T}(E)]dE \tag{1}$$

and

$$S = \frac{2e^2}{h}\int_{\mu_R}^{\mu_L} \mathrm{Tr}[\hat{T}(E) - \hat{T}^2(E)]dE, \tag{2}$$

where $\hat{T}(E)$ is the transmission matrix at energy $E$. It is known that the computation of disorder averaged current/conductance and shot noise involve the average of different two-GF correlators, such as $G^A\Gamma G^R$ for $\hat{T}$, and $G^<\Gamma G^<$ for $\hat{T}^2$, where $G^{R/A/<}$ are the retarded, advanced and "lesser" Green's function, $\Gamma$ is the linewidth function of the electrode [42,43]. Generally, the average of any two-GF correlator requires including the effect of multiple impurity scattering processes that correlate the two propagators, giving rise to the vertex corrections. The generalized CPA-NVC method derives nine NVCs to account for the disorder scattering at nonequilibrium condition, providing a complete VC set for averaging any two-GF correlator. As a result, the disorder average of any two-GF correlator consists of coherent and vertex correction parts. The generalized CPA-NVC method provides a unified and effective way to obtain various transport properties, including the averaged nonequilibrium density matrix, averaged current/transmission, shot noise, and device-to-device property which involve different two-GF correlators [42,43]. In combination with first-principles method, the effect of disordered impurities/defects on the transport statistics of a nanoscale device can be analyzed from first principles. In this paper, we apply the first-principles generalized CPA-NVC to study effects of different types of disorders on the spin dependent conductance, shot noise, and tunneling magnetoresistance in symmetric and asymmetric DBMTJs.

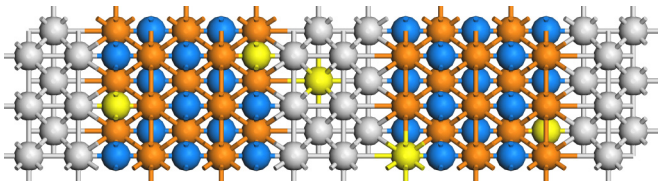

FIG. 1. Schematic structure of MgO-based DBMTJ. The grey, blue, orange, yellow spheres represent Fe, oxygen, Mg, and defects, respectively. The electrodes extend to infinity.

Figure 1 presents a schematic structure of a DBMTJ with two MgO-barrier containing atomic disorders. In our simulation, the disorder is modeled by an alloy model $A_{1-x}B_x$ with $x$ denoting the concentration of atom $B$. We mainly investigate the symmetric DBMTJ with a symmetric barrier of five-monolayer (ML) MgO and the asymmetric DBMTJ with 5- and 7-ML MgO barriers (denoted as MTJ5-5 and MTJ5-7, respectively.). We consider 4-ML Fe in the middle FM layer because it is representative in the ultrathin regime and has no strong coupling between the two interfacial Fe layers. To demonstrate the important effects of interfacial disorder on modulating the spin dependent tunneling, we consider two types of distinct disorders including oxygen vacancies (OVs) in the MgO barrier, and Fe vacancies (FeV) in the middle Fe layer with disorder concentration $x$ ranging from 0.2% to 10%. In all our electronic structure calculations, the Von Barth-Hedin form of local spin density approximation is employed for the exchange-correlation functional [46]. We use $60 \times 60$ and $400 \times 400$ $k$ meshes in the Brillouin zone (BZ) to converge the electronic structure and transport properties, respectively.

## II. SPIN DEPENDENT CONDUCTANCE

In this section, we investigate the effects of disorder on the spin dependent tunneling in four different magnetic configurations of DBMTJs, including a parallel state $P(\uparrow\uparrow\uparrow)$ and three different antiparallel states of $AP1(\uparrow\downarrow\uparrow)$, $AP2(\uparrow\downarrow\downarrow)$, and $AP3(\uparrow\uparrow\downarrow)$ with arrows from left to right denoting the magnetization direction of the left electrode, middle layer, and right electrode (please note that the states AP2 and AP3 are equivalent in MTJ5-5). In Fig. 2, we plot the total conductance and its coherent and vertex correction parts for the majority- and minority-spin channels (defined with Fe in the right electrode) in different magnetic configurations. Figures 2(a)–2(c) present the results for P, AP1, and AP2 states of MTJ5-5 containing the same OV concentration $x$ on each interfacial MgO layer (denoted as $\mathcal{G}_P$, $\mathcal{G}_{AP1}$, and $\mathcal{G}_{AP2}$, respectively). It is clearly seen that disordered interfacial OVs

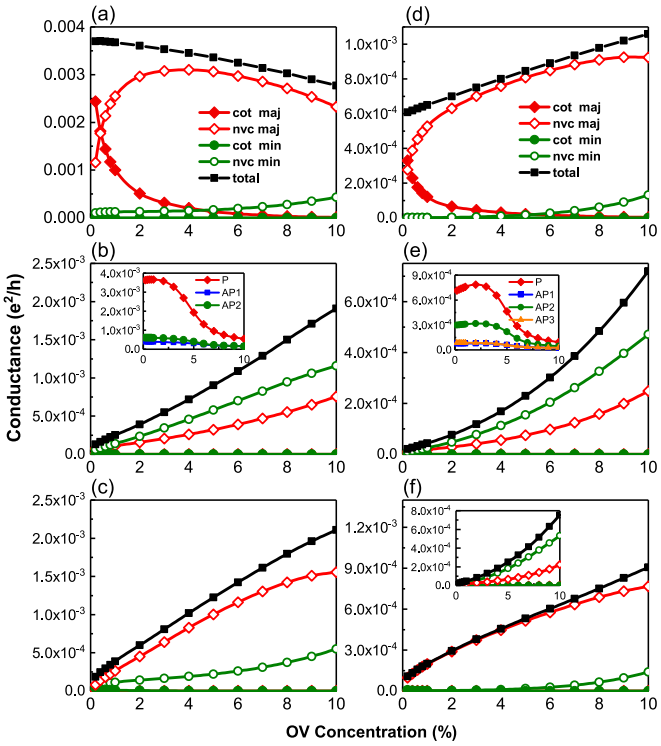


FIG. 2. Disorder dependence of conductance for different magnetic states of DBMTJs. Panels (a)–(c) present spin-resolved and total conductances vs interfacial OV $x$ for P(↑↑↑), AP1(↑↓↑), and AP2(↑↓↓) states of MTJ5-5, respectively. Panels (d)–(f) and inset of (f) present the results for P(↑↑↑), AP1(↑↓↑), AP2(↑↓↓), and AP3(↑↑↓) of MTJ5-7. The insets of (b) and (e) represent total conductances vs middle-layer FeV $x$ with 2% interfacial OVs for different magnetic states in MTJ5-5 and MTJ5-7, respectively.

play a significant role in all the spin channels. Importantly, the presence of interfacial disorder substantially enhances the total $\mathcal{G}_{AP1}$ and $\mathcal{G}_{AP2}$ to become even comparable with $\mathcal{G}_P$ which is slightly reduced by increasing the disorder $x$, presenting the important effects of interfacial disorder scattering. For example, for OVs $x = 2\%$, $\mathcal{G}_{AP1} = 3.9 \times 10^{-4} e^2/h$ and $\mathcal{G}_{AP2} = 6.0 \times 10^{-4} e^2/h$, significantly larger than the values $\mathcal{G}_{AP1} = 1.3 \times 10^{-4} e^2/h$ and $\mathcal{G}_{AP2} = 1.86 \times 10^{-4} e^2/h$ at $x = 0.2\%$.

The conductance results versus interfacial OV $x$ for MTJ5-7 are shown in Figs. 2(d)–2(f) and the inset of 2(f) for the respective four magnetic states of P, AP1, AP2, and AP3. In contrast to the decrease of $\mathcal{G}_P$ in the symmetric MTJ5-5 as shown in Fig. 2(a), $\mathcal{G}_P$ of the asymmetric MTJ5-7 is increased with increasing interfacial OVs, presenting a different effect of interfacial disorder. However, $\mathcal{G}_{AP1}$, $\mathcal{G}_{AP2}$, and $\mathcal{G}_{AP3}$ of MTJ5-7 present a quite similar dependence on the interfacial OVs to that of MTJ5-5, but their magnitudes are reduced significantly by the 2-ML thicker MgO barrier. Due to the asymmetry in MTJ5-7, AP2 and AP3 are not equivalent. As shown in the inset of Fig. 2(f), the asymmetry significantly reduces the magnitude of $\mathcal{G}_{AP3}$ in comparison with that of $\mathcal{G}_{AP2}$. For example, the ratio $\mathcal{G}_{AP3}/\mathcal{G}_{AP2} = 0.287$ at $x = 2\%$ in MTJ5-7 compared to the unity in MTJ5-5. However, in the meanwhile, the relative difference between AP1 and AP3 is greatly reduced in MTJ5-7 compared to that in MTJ5-5. In MTJ5-7, the junction resistance is mainly determined by the part with 7-ML MgO, giving rise to the small difference between AP1 and AP3.

In the inset of Figs. 2(b) and 2(e), we investigate the effects of disordered Fe vacancies in middle Fe layer of MTJ5-5 and MTJ5-7 with 2% OVs on the interfaces. It is clear that FeVs have a limited effect on the total conductance of all magnetic states at low concentration but strong suppression on $\mathcal{G}_P$ at high concentration. Therefore, for low concentration disorder, the interfacial OVs play a critical role in the spin-dependent tunneling in DBMTJ, and thus determine the transport property of the device.

As shown in Fig. 2, the interfacial disordered OVs present significant effects on the spin dependent tunneling in different magnetic states of MTJ5-5 and MTJ5-7. It is observed that, for $\mathcal{G}_P$, the presence of interfacial disorder quickly suppresses the contribution of the coherent part, and enhances the vertex correction part to quickly become dominant. Moreover, the conductances of both spin channels in AP1, AP2, AP3 and the minority-spin channel of P are all dominated by the vertex correction part with monotonic increase with increasing the disorder $x$. As known, the vertex correction part accounts for the contribution of disorder induced interchannel scattering. Generally, the presence of interfacial disorder lifts the limitation of symmetry conservation that is required for tunneling in a perfect device, and thus allows the electron to tunnel through new channels formed by the interchannel scattering, giving rise to both constructive and destructive effects of disorder.

Figure 3 presents the $\mathbf{k}_\parallel$-resolved transmission function $T(\mathbf{k}_\parallel) = \mathbf{Tr}[\bar{\mathbf{T}}(\mathbf{k}_\parallel)]$ (the overbar denotes disorder average) for the spin channels dominating different magnetic states of MTJ5-5 (left) and MTJ5-7 (right) with interfacial OVs $x = 0.002$, 0.01, 0.05, and 0.10. It is apparent that, with increasing the disorder, the patterns of $T(\mathbf{k}_\parallel)$ in all magnetic configurations become more and more diffusive, illustrating the effects of interchannel scattering. For the majority spin of the P state in MTJ5-5, at $x = 0.002$, it is clear that the dominant contribution to conductance is the coherent resonant tunneling, namely the hot ring around the BZ center in Fig. 3(a) on the left. However, as known, diffusive scattering induces the destructive interference that enhances backscattering, eliminating coherent resonant tunneling channels [47]. As a consequence, $\mathcal{G}_{P,\mathrm{maj}}$ is decreased with increasing interfacial disorder due to a quickly suppressed contribution of coherent resonant tunneling as shown in Fig. 2(a), in contrast to the results of all the other spin channels.

From Fig. 3(a) on the right for $x = 0.002$, we can see that the increase of 2-ML MgO on one barrier side greatly reduces the transmission magnitude compared to the result of MTJ5-5, substantially suppressing the contribution of the resonant tunneling process. This is because the two more monolayer MgO in MTJ5-7 can effectively reduce the coupling of the electronic states from left and right electrodes that is required for effective resonant tunneling [48,49]. For the electrons with low transmission in a perfect tunnel junction, disorder induced interchannel scattering can couple the electrons to tunneling channels with higher transmission, exponentially increasing the transmission of the electron. The increase of disorder increases the strength of interchannel scattering, and thus

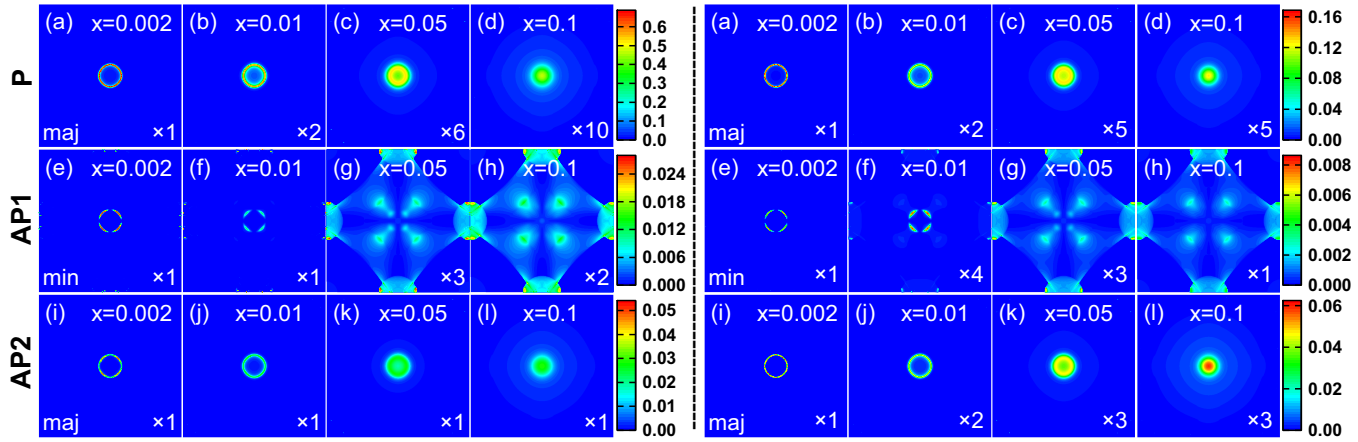


FIG. 3. $\mathbf{k}_\parallel$-resolved transmission for the dominating spin channels in P, AP1, and AP2 states of MTJ5-5 (left) and MTJ5-7 (right) with interfacial OVs $x = 0.002$, 0.01, 0.05, and 0.10. Here, $\mathbf{k}_\parallel \in [-\frac{\pi}{a}, \frac{\pi}{a}] \times [-\frac{\pi}{a}, \frac{\pi}{a}]$, where $a$ is the lattice constant in the plane perpendicular to the transport direction. The scaling factor is given on the right-bottom corner for each subset.

enhances the coupling between different channels. Therefore, we can find that the presence of disorder enhances the transmission in a wide range of BZ (Fig. 3), presenting the constructive effect of interchannel scattering. As a consequence, the total conductance of all the AP states and P states of MTJ5-7 can be substantially increased with increasing the interfacial disorder $x$. We have seen that disorder induced interchannel scattering can play dominant roles in the transmission of all spin channels. However, understanding of the disorder effects on the nature of transport channels and tunneling statistics cannot be obtained by only analyzing the transmission, and thus requires further study of shot noise.

## III. TUNNELING MAGNETORESISTANCE

We have shown the significant modulation on the spin dependent conductance by disorders and asymmetry in the MgO based DBMTJ. Here, we investigate the disorder and asymmetry effects on the TMR, which is defined as $\mathrm{TMR}_{AP} = (\mathcal{G}_P - \mathcal{G}_{AP})/\mathcal{G}_{AP}$. Figure 4 presents TMR results for different antiparallel magnetic states in MTJ5-5 and MTJ5-7. Similar to the effects of interfacial OVs in single barrier MTJ [32,35],

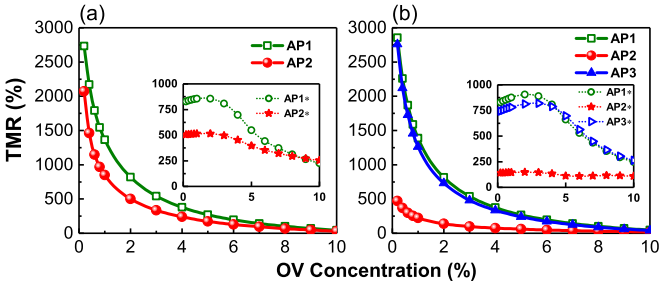


FIG. 4. Disorder dependence of TMR for different antiparallel magnetic states. Panels (a) and (b) present TMR vs interfacial OV $x$ for MTJ5-5 and MTJ5-7, respectively. The insets of (a) and (b) present TMR vs middle-layer FeV $x$ for MTJ5-5 and MTJ5-7 with 2% interfacial OVs, respectively. The green, red, and blue symbols represent TMRs for AP1(↑↓↑), AP2(↑↓↓), and AP3 (↑↑↓), respectively.

interfacial OVs in DBMTJ can substantially reduce the TMR value for all the AP states due to the significant enhancement in their transmissions as shown in Fig. 2. For example, with $x = 2\%$ OVs, for MTJ5-5, $\mathrm{TMR}_{AP1}$ and $\mathrm{TMR}_{AP2}$ are reduced to 820% and 500% from the corresponding values 2750%, 1880% at $x = 0.2\%$; for MTJ5-7, $\mathrm{TMR}_{AP1} = 810\%$ and $\mathrm{TMR}_{AP2} = 140\%$ while their values at $x = 0.2\%$ are 2860% and 470%, respectively. As another important effect of interfacial OVs, the difference between $\mathrm{TMR}_{AP1}$ and $\mathrm{TMR}_{AP2}$ is becoming smaller and smaller with the disorder $x$ increasing and become almost negligible above $x = 6\%$ for both MTJ5-5 and MTJ5-7. However, DBMTJs with low concentration of interfacial OVs still present giant TMR effects and the difference between TMR values of AP1 and AP2 is still appreciable, presenting multiple resistance states for applications in memory. It should be mentioned that, without considering the contribution of the interchannel scattering, namely the vertex correction part, the TMR values are totally wrong in both magnitude and dependence on disorders.

Furthermore, the TMR difference between AP1 and AP2 of MTJ5-7 is significantly enlarged in comparison with MTJ5-5, for example, the ratio $\mathrm{TMR}_{AP1}/\mathrm{TMR}_{AP2}$ is 5.79 while it is 1.64 for MTJ5-5 at $x = 2\%$, presenting an important consequence of the asymmetry. We also note that, due to the asymmetry in MTJ5-7, the TMR of AP3 are very different from the value of AP2 (note AP2 and AP3 are equivalent in MTJ5-5), but is very close to the value of AP1. It can be seen that as further increasing the asymmetry, the difference between the resistance of AP3 and AP1 become smaller and smaller. As a result, MTJ5-7 or more asymmetric DBMTJ still presents two antiparallel magnetic states with appreciable difference, same as the symmetric MTJ5-5. The insets of Fig. 4 present the TMR values for MTJ5-5 and MTJ5-7 with FeV and 2% interfacial OVs. It is found that FeVs change the TMR values in a limited way compared to the effects of interfacial OVs and asymmetry enlarges the difference between AP1 and AP2. Similar to OVs, the increase of FeVs reduces the difference between TMR values of AP1 and AP2. Therefore, in both the symmetric and asymmetric DMTJs, the interfacial disorders play a determinant role in the spin dependent tunneling.

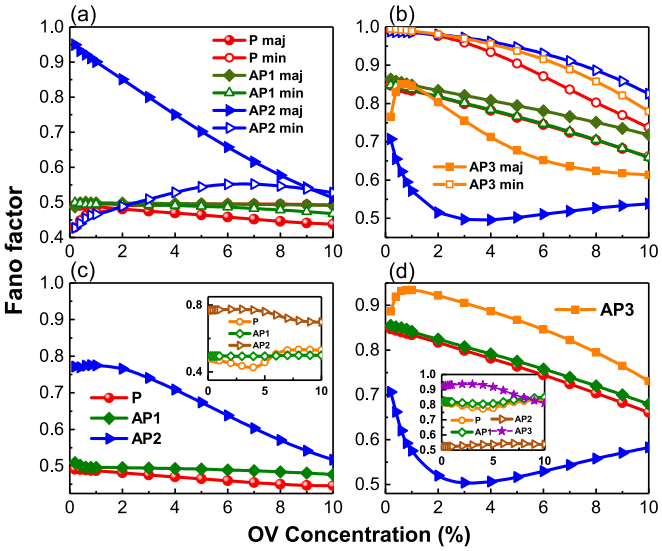


FIG. 5. Disorder dependence of Fano factor in different magnetic states. Panels (a) and (b) present spin-resolved Fano factor vs interfacial OV $x$ for MTJ5-5 and MTJ5-7, respectively. Panels (c) and (d) present total Fano factor vs interfacial OV $x$ for different magnetic states in MTJ5-5 and MTJ5-7, respectively. The insets of (c) and (d) represent Fano factor versus middle-layer FeV $x$ for MTJ5-5 and MTJ5-7, respectively. The solid and vacant symbols represent the respective majority- and minority-spin channels.

## IV. SPIN DEPENDENT SHOT NOISE

Further understanding the spin dependent tunneling process requires the second cumulant shot noise to obtain more information. Generally, in the noninteracting transport regime, the low transmission channel, such as the normal tunneling channel, presents a high Fano factor, featuring the uncorrelated Poissonian process. However, the high-transmission channel, such as the resonant tunneling channel, presents a significantly suppressed Fano factor, reflecting the important effects of correlation arising from Pauli principle due to high occupation of the channel [27,28]. Thus, the Fano factor can be used to detect the nature of transport channels, and reflect the correlation induced by Pauli principle. In the following, we study the Fano factor $F = S/2e\mathcal{G}$ to reveal the nature of tunneling channels. In Fig. 5, we show the spin-resolved Fano factors versus OV disorder $x$ for MTJ5-5 and MTJ5-7 in (a) and (b), and the total Fano factors in (c) and (d).

For symmetric MTJ5-5, as seen from Fig. 5(a), Fano factors for the two spin channels of the P and AP1 with symmetric magnetic states all remain close to 0.5 with different interfacial disorder $x$, agreeing well with previous theoretical predictions for symmetric double-barrier junctions [26,27,50–52] (the slight suppression below 0.5 for $F_{P,\mathrm{min}}$ at low $x$ and $F_{P,\mathrm{maj}}$ at high $x$ is consistent with a previous report [53]). Therefore, although interfacial disordered OVs can significantly affect the tunneling conductance and TMR, the tunneling statistics in P and AP1 of MTJ5-5 remains almost unchanged by the interchannel scattering of interfacial disordered OVs. However, for AP2 of MTJ5-5, due to the asymmetry in the spin dependent electronic structure, the Fano factors of majority- and minority-spin behave very differently from each other, and deviate from the value 0.5, presenting different tunneling statistics from P and AP1 magnetic states. In particular, for AP2, $F_{AP2,\mathrm{maj}}$ presents small suppression from unity at low concentration, such as $F_{AP2,\mathrm{min}} = 0.95$ at $x = 0.002$, which is significantly higher than 0.5, reflecting the Poissonian dominated process. In the meanwhile, $F_{AP2,\mathrm{min}}$ is substantially suppressed and remains between 0.42 and 0.55 as $x$ changes, revealing the significant sub-Poissonian tunneling process in contrast to the majority spin channel of AP2. However, with increasing $x$, $F_{AP2,\mathrm{maj}}$ can be significantly decreased to become as low as 0.52 at $x = 10\%$, presenting significant sub-Poissonian tunneling statistics induced by interfacial disorder. Such an important suppression in $F_{AP2,\mathrm{maj}}$ is due to the increased contribution of tunneling through high-transmission channels (formed by disorder induced interchannel scattering) featuring low Fano factor.

As shown in Fig. 5(b), the spin-resolved Fano factors of MTJ5-7 present large differences in comparison with the results of MTJ5-5, presenting the important effect of asymmetry on the tunneling statistics. In particular, for both spin channels in P and AP1 states of MTJ5-7, the Fano factors present important deviation from the value close to 0.5 as observed in the MTJ5-5. For example, at $x = 0.002$, $F_{P,\mathrm{maj}} = 0.85$, $F_{AP1,\mathrm{min}} = 0.85$, $F_{AP1,\mathrm{maj}} = 0.86$ are significantly enhanced over that of MTJ5-5. At the same time, $F_{AP2,\mathrm{min}}$ is enhanced to 0.99 from the value 0.43 of MTJ5-5, and $F_{AP2,\mathrm{maj}}$ is suppressed to 0.71 from the value 0.95 of MTJ5-5, presenting distinct effects of asymmetry on modulating the spin dependent tunneling statistics. The enhanced Fano factor in MTJ5-7 implies the reduction or even elimination of resonant tunneling channels compared to that in MTJ5-5, making the tunneling more Poissonian, or uncorrelated. As an important effect of interfacial disorder, for most of the spin channels, the Fano factor is decreased with increasing $x$. The most dramatic effect of interfacial disorder is found in $F_{AP2,\mathrm{maj}}$ which presents a fast decrease to the minimum of 0.5 at $x = 4\%$ followed by a slow increase. Similar to the $F_{AP2,\mathrm{maj}}$ of MTJ5-5, the decrease of the Fano factor in MTJ5-7 can be attributed to the enhanced ratio of high-transmission channel contribution to the total.

The insets of Figs. 5(c) and 5(d) present the total Fano factor versus central FeVs $x$ for MTJ5-5 and MTJ5-7 with 2% interfacial OVs. It is clear that all the Fano factors can only be slightly modulated by FeVs, implying the small effect of central FeVs on the spin dependent tunneling statistics. Therefore, the tunneling statistics in different spin channels are mainly determined by the interfacial disorders and barrier asymmetry of the junction, and disorder in the middle Fe layer takes limited effects on the spin dependent tunneling in DBMTJs.

In Fig. 6, we investigate the $k$-resolved Fano factor defined as $F(\mathbf{k}_\parallel) = \mathrm{Tr}[\overline{\hat{\mathbf{T}}}(\mathbf{k}_\parallel) - \overline{\hat{\mathbf{T}}^2}(\mathbf{k}_\parallel)]/\mathrm{Tr}[\overline{\hat{\mathbf{T}}}(\mathbf{k}_\parallel)]$ for the dominating spin channels in different magnetic states of MTJ5-5 with interfacial OVs $x = 0.002$, 0.01, 0.05, and 0.10. The value of $F(\mathbf{k}_\parallel)$ reveals the tunneling statistics of the incoming electron with the wave vector $\mathbf{k}_\parallel$. For a wide range of $\mathbf{k}_\parallel$, it is found that the increase of disorder reduces the $F(\mathbf{k}_\parallel)$ for all spin channels plotted for MTJ5-5. Most apparently, $F(\mathbf{k}_\parallel)$ of the majority spin channel of AP2 can be quickly reduced from above 0.9 at $x = 0.002$ to about 0.5 at $x = 0.1$. It is notable that $F(\mathbf{k}_\parallel)$ of minority spin of AP1 is only slightly reduced,

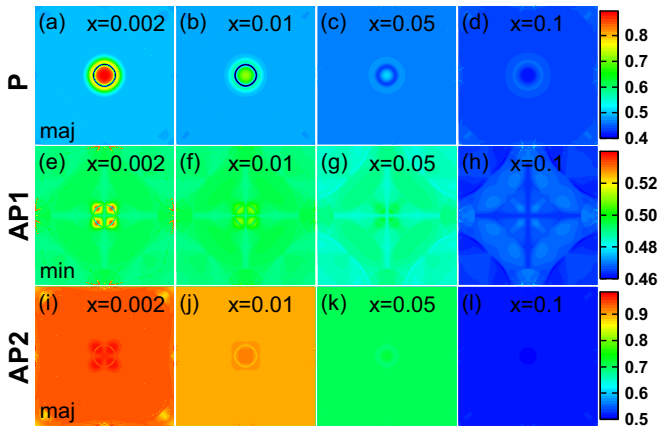


FIG. 6. $\mathbf{k}_\parallel$-resolved Fano factor in the first Brillouin zone for the dominating spin channels in P, AP1, and AP2 states of MTJ5-5 with OV $x = 0.002$, 0.01, 0.05, and 0.10.

and remains close to 0.5 at each $\mathbf{k}_\parallel$ in the BZ. However, for the majority-spin channel of P, we find that, in the red circle region with high transmission as shown in Fig. 3(a) (left), $F(\mathbf{k}_\parallel)$ is enhanced from the value close to 0.4 at $x = 0.002$ to above 0.5 at $x = 0.1$ while the corresponding $T(\mathbf{k}_\parallel)$ is reduced, revealing the important destructive effect of disorder on coherent resonant tunneling channels.

Figure 7 plots the $F(\mathbf{k}_\parallel)$ for the dominating spin channels in MTJ5-7. Similar to the results of MTJ5-5, the increase of interfacial disorder reduces $F(\mathbf{k}_\parallel)$ with increased $T(\mathbf{k}_\parallel)$ in most areas of the BZ for all spin channels in MTJ5-7 as shown in Fig. 7. However, except the AP2, the Fano factors of P, AP1, AP3 of MTJ5-7 presented in Fig. 7 are significantly enhanced compared to the results of MTJ5-5 in Fig. 6. In particular, for the majority spin of P in MTJ5-7 at $x = 0.1$, $F(\mathbf{k}_\parallel)$ is about the value 0.7 while it is close to 0.5 in MTJ5-5. Such an increase

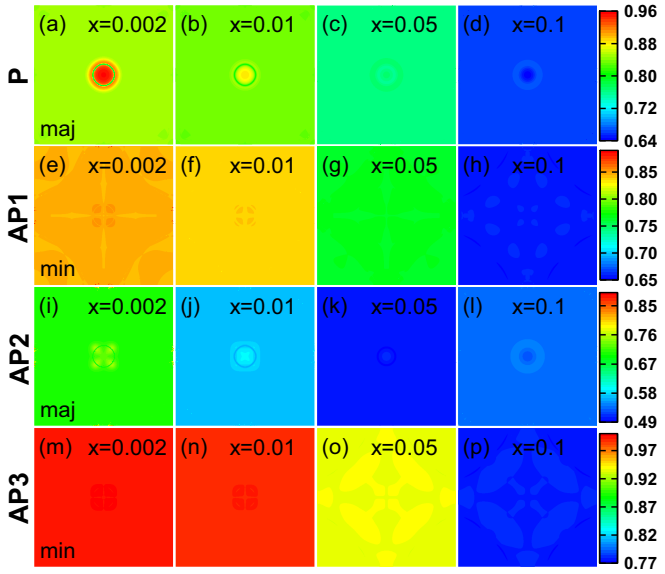


FIG. 7. $\mathbf{k}_\parallel$-resolved Fano factor in the first Brillouin zone for the dominating spin channels in P, AP1, AP2, and AP3 states of MTJ5-7 for OV $x = 0.002$, 0.01, 0.05, and 0.10.

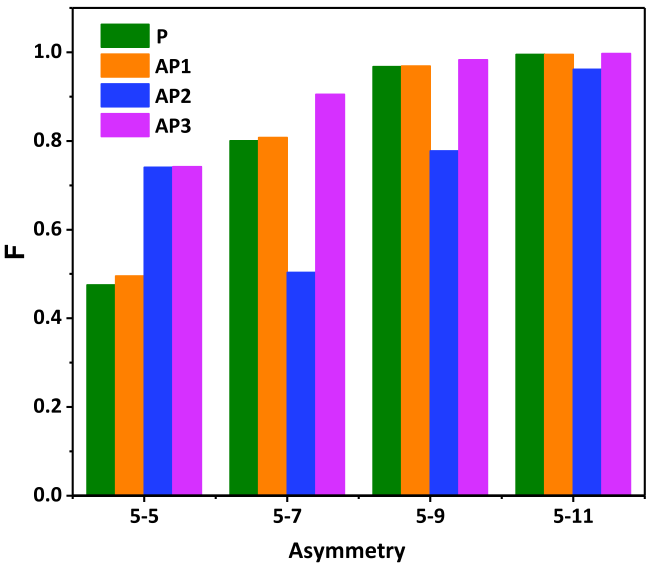


FIG. 8. Barrier asymmetry dependence of the Fano factor in different magnetic states. 5-5, 5-7, 5-9, 5-11 represent MTJ5-5, MTJ5-7, MTJ5-9, MTJ5-11 with 3% interfacial OVs, respectively.

in $F(\mathbf{k}_\parallel)$ of MTJ5-7 reveals that the contribution of high-transmission channels to the total is reduced in comparison with that in MTJ5-5, reflecting the decreased coupling between the electronic states of electrodes in MTJ5-7. We note that the increased $T(\mathbf{k}_\parallel)$ in Fig. 3 corresponds to the reduced Fano factor $F(\mathbf{k}_\parallel)$ in Figs. 6 and 7 in a wide range of BZs. The increase of disorder increases the coupling of the electrons to the existing high-transmission tunneling channels, resulting in a higher transmission with a lower Fano factor. As an important feature of disorder effects on the $k$-resolved Fano factor, the increase of interchannel scattering uniformize the $F(\mathbf{k}_\parallel)$ in the whole BZ as seen from Figs. 6 and 7, eliminating the symmetry dependence.

To further investigate the asymmetry effects on tunneling statistics, we calculate another two MTJs including MTJ5-9 and MTJ5-11 with 3% interfacial OVs and compare the Fano factor results in Fig. 8. It is clear that, at the very asymmetric MTJ5-11, all the Fano factors are all very close to unity, presenting the Poissonian dominated statistics. Therefore, as the asymmetry increases, the correlation induced by Pauli principle can be significantly decreased, and become even negligible in MTJ5-11. It is notable that, for all the asymmetric DBMTJ calculated in Fig. 8, $F_{AP2}$ presents an important suppression compared to other magnetic states. Starting from MTJ5-7, all the Fano factors increase monotonically to finally reach unity. Compared to the symmetric DBMTJ, increasing barrier thickness on one side in the asymmetric DBMTJ exponentially reduce the effective coupling of the states in two electrodes that is required for the formation of high-transmission channels. As a result, the contribution of high-transmission channels can be quickly decreased and finally eliminated, enhancing the Fano factor and finally resulting in the Poissonian dominated process in the very asymmetric junctions. Our observations on the effects of asymmetry are consistent with the experimental measurement [25].

To check if our conclusion on the disorder effects of interfacial OVs and FeVs is generally applicable, we carried out calculations for DBMTJs with 8-ML Fe in the middle FM layer. We found that the disorder induced interchannel scattering (by interfacial OVs or FeVs) plays similar roles in spin dependent tunneling in DBMTJs with 4- and 8-ML Fe in the middle FM layer. The thickness of the middle Fe layer affects the specific value of spin dependent conductance, magnetoresistance, and shot noise, but does not change the general effects of interchannel scattering induced by interfacial OVs and FeVs on the tunneling statistics in DBMTJs.

## V. CONCLUSION

We have carried out first-principles study of the effects of different modulations on the shot noise and tunneling magnetoresistance in Fe/MgO/Fe/MgO/Fe double-barrier magnetic tunneling junctions, including interfacial oxygen vacancies, Fe vacancies in middle layer, and the barrier asymmetry. It is found that the presence of interfacial disorder favors the sub-Poissonian tunneling process in different magnetic states of the junction. As an important consequence, the Fano factors of the junction with symmetric barrier maintain around the value of 0.5 or can be decreased by interfacial oxygen vacancies, while all Fano factors of asymmetric junctions can be significantly suppressed. The suppressed shot noise reflects the enhanced contribution of high-transmission channels formed by interchannel scattering, reflecting the increased correlation due to Pauli principle. Moreover, the interchannel scattering by interfacial oxygen vacancies can dramatically reduce the TMR by significantly enhancing the transmission of antiparallel magnetic states. Compared to the interfacial oxygen vacancies, Fe vacancies in the middle layer have limited effects on the shot noise. In addition, The increase of the barrier asymmetry exponentially reduces the effective coupling of states from electrodes, quickly decreasing high-transmission channels to finally present Poissonian dominated process in the very asymmetric junctions.

## ACKNOWLEDGMENTS

Y.K. acknowledges the financial support from the ShanghaiTech University start-up fund, "The Thousand Young Talents Plan" and Shanghai "Shuguang Plan."

[1] J. S. Moodera, L. R. Kinder, T. M. Wong, and R. Meservey, Phys. Rev. Lett. **74**, 3273 (1995).
[2] S. S. P. Parkin, C. Kaiser, A. Panchula, P. M. Rice, B. Hughes, M. Samant, and S. H. Yang, Nat. Mater. **3**, 862 (2004).
[3] S. Yuasa, T. Nagahama, A. Fukushima, Y. Suzuki, and K. Ando, Nat. Mater. **3**, 868 (2004).
[4] S. Ikeda, J. Hayakawa, Y. Ashizawa, Y. M. Lee, K. Miura *et al.*, Appl. Phys. Lett. **93**, 082508 (2008).
[5] R. W. Dave, G. Steiner, J. M. Slaughter, and J. J. Sun, IEEE Trans. Magn. **42**, 1935 (2006).
[6] W. H. Butler, X.-G. Zhang, T. C. Schulthess, and J. M. MacLaren, Phys. Rev. B **63**, 054416 (2001).
[7] X. Zhang, B. Z. Li, G. Sun, and F. C. Pu, Phys. Rev. B **56**, 5484 (1997).
[8] T. Nozaki, N. Tezuka, and K. Inomata, Phys. Rev. Lett. **96**, 027208 (2006).
[9] S. Yuasa, T. Nagahama, and Y. Suzuki, Science **297**, 234 (2002).
[10] N. Zou and K. A. Chao, Phys. Rev. Lett. **69**, 3224 (1992).
[11] R. S. Liu, S. H. Yang, X. Jiang, X.-G. Zhang, C. Rettner *et al.*, Phys. Rev. B **87**, 024411 (2013).
[12] M. M. Glazov, P. S. Alekseev, M. A. Odnoblyudov, V. M. Chistyakov, S. A. Tarasenko, and I. N. Yassievich, Phys. Rev. B **71**, 155313 (2005).
[13] A. G. Petukhov, A. N. Chantis, and D. O. Demchenko, Phys. Rev. Lett. **89**, 107205 (2002).
[14] S. Colis, G. Gieres, L. Bar, and J. Wecker, Appl. Phys. Lett. **83**, 948 (2003).
[15] T. Nozaki, A. Hirohata, N. Tezuka, S. Sugimoto, and K. Inomata, Appl. Phys. Lett. **86**, 082501 (2005).
[16] J. Peralta-Ramos, A. M. Llois, I. Rungger, and S. Sanvito, Phys. Rev. B **78**, 024430 (2008).
[17] G. Feng, S. V. Dijken, and J. M. D. Coey, Appl. Phys. Lett. **89**, 162501 (2006).
[18] G. Feng, S. van Dijken, J. F. Feng, J. M. D. Coey, T. Leo, and D. J. Smith, J. Appl. Phys. **105**, 033916 (2009).
[19] R. Daqiq and N. Ghobadi, Superlattices Microstruct. **102**, 417 (2017).
[20] Z. Diao, A. Panchula, Y. Ding, M. Pakala, S. Wang *et al.*, Appl. Phys. Lett. **90**, 132508 (2007).
[21] I. Theodonis, A. Kalitsov, and N. Kioussis, Phys. Rev. B **76**, 224406 (2007).
[22] A. Iovan, S. Andersson, Y. G. Naidyuk, A. Vedyaev, B. Dieny *et al.*, Nano Lett. **8**, 805 (2008).
[23] A. N. Useinov, J. Kosel, N. K. Useinov, and L. R. Tagirov, Phys. Rev. B **84**, 085424 (2011).
[24] Z. P. Niu, Z. B. Feng, J. Yang, and D. Y. Xing, Phys. Rev. B **73**, 014432 (2006).
[25] J. P. Cascales, D. Herranz, F. G. Aliev, T. Szczepański, V. K. Dugaev, J. Barnas, A. Duluard, M. Hehn, and C. Tiusan, Phys. Rev. Lett. **109**, 066601 (2012).
[26] T. Szczepański, V. K. Dugaev, J. Barnaś, J. P. Cascales, and F. G. Aliev, Phys. Rev. B **87**, 155406 (2013).
[27] Y. M. Blanter and M. Büttiker, Phys. Rep. **336**, 1 (1999).
[28] C. Beenakker and C. Schnenberger, Phys. Today **56**(5), 37 (2003).
[29] D. L. Li, J. F. Feng, G. Q. Yu, P. Guo, J. Y. Chen *et al.*, J. Appl. Phys. **114**, 213909 (2013).
[30] F. Bonell, S. Andrieu, A. M. Bataille, C. Tiusan, and G. Lengaigne, Phys. Rev. B **79**, 224405 (2009).
[31] S. Z. Wang and K. Xia, Phys. Rev. B **93**, 184414 (2016).
[32] G. X. Miao, Y. J. Park, J. S. Moodera, M. Seibt, G. Eilers, and M. Münzenberg, Phys. Rev. Lett. **100**, 246803 (2008).
[33] A. Kalitsov, P. J. Zermatten, F. Bonell, G. Gaudin, S. Andrieu *et al.*, J. Phys.: Condens. Matter **25**, 496005 (2013).
[34] K. D. Belashchenko, E. Y. Tsymbal, M. van Schilfgaarde, D. A. Stewart, I. I. Oleinik, and S. S. Jaswal, Phys. Rev. B **69**, 174408 (2004).

[35] Y. Ke, K. Xia, and H. Guo, Phys. Rev. Lett. **105**, 236801 (2010).
[36] J. M. Teixeira, J. Ventura, J. P. Araujo, J. B. Sousa, P. Wisniowski, S. Cardoso, and P. P. Freitas, Phys. Rev. Lett. **106**, 196601 (2011).
[37] D. Waldron, V. Timoshevskii, Y. Hu, K. Xia, and H. Guo, Phys. Rev. Lett. **97**, 226802 (2006).
[38] X.-G. Zhang, W. H. Butler, and A. Bandyopadhyay, Phys. Rev. B **68**, 092402 (2003).
[39] J. Yan, S. Wang, K. Xia, and Y. Ke, Phys. Rev. B **97**, 014404 (2018).
[40] K. Liu, K. Xia, and G. E. W. Bauer, Phys. Rev. B **86**, 020408 (2012).
[41] Y. Ke, K. Xia, and H. Guo, Phys. Rev. Lett. **100**, 166805 (2008).
[42] J. Yan and Y. Ke, Phys. Rev. B **94**, 045424 (2016).
[43] J. Yan, S. Wang, K. Xia, and Y. Ke, Phys. Rev. B **95**, 125428 (2017).
[44] P. Soven, Phys. Rev. **156**, 813 (1967).
[45] D. W. Taylor, Phys. Rev. **156**, 1029 (1967).
[46] U. von Barth and L. Hedin, J. Phys. C **5**, 1629 (1972).
[47] P. W. Anderson, Phys. Rev. **109**, 1492 (1958).
[48] C. Tiusan, J. Faure-Vincent, C. Bellouard, M. Hehn, E. Jouguelet, and A. Schuhl, Phys. Rev. Lett. **93**, 106602 (2004).
[49] O. Wunnicke, N. Papanikolaou, R. Zeller, P. H. Dederichs, V. Drchal, and J. Kudrnovský, Phys. Rev. B **65**, 064425 (2002).
[50] M. de Jong and C. Beenakker, Physica A **230**, 219 (1996).
[51] L. Y. Chen and C. S. Ting, Phys. Rev. B **43**, 4534 (1991).
[52] M. Büttiker, Physica B **175**, 199 (1991).
[53] V. Ya Aleshkin *et al.*, Semicond. Sci. Technol. **19**, 665 (2004).